PROTEINS
STRUCTURE ■ FUNCTION ■ BIOINFORMATICS

Universality of protein reentrant condensation in solution induced by multivalent metal ions

Fajun Zhang,[1]* Sophie Weggler,[2] Michael J. Ziller,[1] Luca Ianeselli,[1] Benjamin S. Heck,[1] Andreas Hildebrandt,[2] Oliver Kohlbacher,[3] Maximilian W. A. Skoda,[4] Robert M. J. Jacobs,[5] and Frank Schreiber[1]

[1] Institut für Angewandte Physik, Eberhard Karls Universität Tübingen, Auf der Morgenstelle 10, Tübingen 72076, Germany
[2] Zentrum für Bioinformatik Saar, Universität des Saarlandes, Im Stadtwald, Building E2.1, Saarbrücken 66123, Germany
[3] Zentrum für Bioinformatik Tübingen, Eberhard Karls Universität Tübingen, Sand 14, Tübingen 72076, Germany
[4] ISIS, Rutherford Appleton Laboratory, Chilton, Didcot OX11 0OX, United Kingdom
[5] Department of Chemistry, Chemistry Research Laboratory, University of Oxford, Mansfield Road, Oxford OX1 3TA, United Kingdom

ABSTRACT

The effective interactions and phase behavior of protein solutions under strong electrostatic coupling conditions are difficult to understand due to the complex charge pattern and irregular geometry of protein surfaces. This distinguishes them from related systems such as DNA or conventional colloids. In this work, we discuss the question of universality of the reentrant condensation (RC) of proteins in solution induced by multivalent counterions, i.e., redissolution on adding further salts after phase separation, as recently discovered (Zhang *et al.*, Phys Rev Lett 2008; 101:148101). The discussion is based on a systematic investigation of five different proteins with different charge patterns and five different multivalent counterions. Zeta potential measurements confirm the effective charge inversion of proteins in the reentrant regime via binding of multivalent counterions, which is supported by Monte Carlo simulations. Charge inversion by trivalent cations requires an overall negative net charge of the protein. Statistical analysis of a representative set of protein sequences reveals that, in theory, this effect could be possible for about half of all proteins. Our results can be exploited for the control of the phase behavior of proteins, in particular facilitating protein crystallization.

Proteins 2010; 78:3450–3457.

Key words: charge inversion; protein condensation; zeta-potential; cation binding on protein surface.

INTRODUCTION

Electrostatic interactions are ubiquitous in colloidal, polyelectrolyte, and biological systems, which determine their stability, phase behavior, gene storage, and replication of DNA and the specific interactions of enzymes *in vivo*.[1–3] Increased interest in this field in the last decades is due in part to the like-charge attraction observed in various systems.[4–6] Theoretical studies and computer simulations have revealed that the electrostatic correlations of multivalent ions can lead to macroion aggregation.[7–13] A phase diagram with a phase separation region, that is, molecular aggregates around the isoelectric point of the macroion with a subsequent restabilization, and redissolution on further increasing salt concentration, called reentrant condensation (RC), was predicted.[10] The RC of polyelectrolyte and DNA in the presence of multivalent counterions are typical examples.[7,14–26]

Proteins are a special type of polyelectrolytes. In contrast to DNA or conventional colloidal systems dominated by same-sign charges, both positive and negative charges coexist on the surface and generally a more complex and more heterogeneous charge pattern prevails, giving rise to significant differences in the interactions. Moreover, globular proteins exhibit a different shape compared with DNA and conventional colloids. The complex surface charge pattern together with various other interactions, such as hydrophobic interaction and hydration, make the phase behavior of protein solutions more complex.[27,28] This complicates the theory immensely and, therefore, a general description for the RC of proteins has yet to be found. In fact, it is not even clear experimentally how common the phenomenon is for proteins. Furthermore, phase behavior of proteins in the presence of iron and aluminum ions may shed light on the mecha-

Additional Supporting Information may be found in the online version of this article.
*Correspondence to: Dr. F. Zhang, Institut für Angewandte Physik, Eberhard Karls Universität Tübingen, Auf der Morgenstelle 10, Tübingen 72076, Germany. E-mail: Fajun.zhang@uni-tuebingen.de.
Received 4 May 2010; Revised 9 July 2010; Accepted 24 July 2010
Published online 19 August 2010 in Wiley Online Library (wileyonlinelibrary.com).
DOI: 10.1002/prot.22852

nism of several diseases, such as Parkinson's and Alzheimer's disease. In both diseases, protein aggregation plays a pivotal role and trivalent metal ions have been implicated in aggregate formation.[29]

Recently, we have reported the first experimental observation of the RC of globular proteins in solution in the presence of multivalent counterions.[6] The universality of the RC phase behavior has direct implications for biomedical applications (e.g., protein crystallization). It has also been found empirically that addition of a small amount of multivalent salts is crucial in many cases for growth of high-quality protein single crystals.[30,31] The strong and specific effects of the multivalent metal ions modify the protein solubility and the fine crystal structure of lysozyme.[32,33]

In this article, we address more general questions related to protein solutions under strong coupling conditions: What are the criteria for predicting the phase behavior in protein solutions? Can the RC behavior be extended to other proteins and other multivalent ions? Is it universal for all proteins? We present a comprehensive picture based on a broad experimental data set and complementary simulations.

MATERIALS AND METHODS

Materials

Proteins were purchased from Sigma-Aldrich: BSA (99%, A3059), HSA (97–99%, A9511), β-Lactoglobulin (90%, L3908), Ovalbumin (98%, A5503), and lysozyme (84,468 units/mg, 62970). Salts used are YCl_3, $AlCl_3$, $FeCl_3$, spermine tetrahydrochloride (Sigma-Aldrich), and $LaCl_3$ (ABCR GmbH, Karlsruhe, Germany). Protein solutions were prepared by diluting a stock solution of 200 mg/mL with aqueous solutions of the respective salts. The phase behavior was determined using laser transmission measurement.[6] Protein secondary structure conservation was determined by FTIR and circular dichroism spectroscopy. Zeta potential measurements were carried out using the zetasizer-Nano from Malvern, which provides a M3-PALS technique for high-resolution zeta potential measurements (Supporting Information).

Monte-Carlo simulations

Experimental evidence (crystal structures, zeta-potential measurements, and phase diagrams) suggests a specific binding of the multivalent counterions to negatively charged side chains. This specific binding can be simulated efficiently using Monte Carlo techniques conceptually similar to methods for predicting protein protonation states.[34] The key assumption is that individual acidic residue (glutamatic and aspartatic acid) side chains on the protein surface can bind one counterion each. The approach is briefly summarized as follows: (1) Proteins are preprocessed to correct for missing atoms, wrong protonation states, and for missing charges. (2) Negatively charged amino acids with solvent-accessible surface contribution are detected and considered as potential binding sites. The overall positive and negative charges are summarized in Table II. (3) As the full computation of the partition function is computationally intractable, a Monte Carlo approach is used to sample it. This is done by randomly generating potential configurations of metal ion binding to protein binding sites and scoring them by a model of the free energy of metal ion binding. (4) From the estimated partition function of the system consisting of the protein and its counterions in water, higher-level quantities can be retrieved. As such, we estimate expected values for the entire charge distribution of the protein at different counterion concentrations (Fig. 3). In particular, we denote $c_{crit}(M^{3+})$ as the counterion concentration in which the effective charge of protein together with bound counterions is zero. Details of the simulation and preparation of protein structures will be published elsewhere.[35]

Sequence data used in the statistical study

The UniRef50 dataset of protein sequences was used as a representative set of the known protein families. In this dataset, no two protein sequences share more than 50% sequence identity. This removes the bias introduced by overrepresentation of well-studied protein families in protein sequence databases. The UniRef50 dataset (version 15.8) was downloaded from the EMBL-EBI website (ftp://ftp.ebi.ac.uk/pub/databases/uniprot/uniref/uniref50/) on September 30, 2009, in FASTA format. The number of acidic (D, E) and basic (K, R) residues was determined from the full protein sequence. Based on the pKa of histidine (H), and neutral pH, the majority of histidines will be unprotonated, it is, therefore, not included for counting the net charge. A protein was considered to have a negative net charge, if the number of acidic residues was larger than the number of basic residues.

RESULTS

Experimental observations

Phase diagram of protein solutions in the presence of multivalent counterions

An overview of the phase behavior of protein solutions in the presence of multivalent salt can be obtained by visual inspection if the protein concentration is high enough. Figure 1 shows a photograph of a series of protein solutions [c(BSA) = 20 mg/mL] with various concentrations of iron(III) chloride. From this series, one can clearly see that, with increasing salt concentration, one crosses a salt concentration threshold c^*, where the protein solutions become turbid due to a phase separation. When further increasing c_{salt} across c^{**}, the solution becomes clear again, that is, the aggregates redissolve. This phenomenon is called RC.[6,36] Over extended

Figure 1
Photograph of BSA at 20 mg/mL with $FeCl_3$ as a function of ionic strength, phase separation occurs between 1 and 2.5 m*M*.

periods of time (many hours to days), the exact positions of c^* and c^{**} become less well defined as the kinetics of aggregation play an important, and yet to be understood, role in the phase behavior. Here, we also note that the secondary structures of the proteins are conserved in the reentrant regime in the presence of multivalent counterions as shown by FTIR and circular dichroism spectroscopy (see Supporting Information).

We have extended the experiments to a number of proteins, such as HSA, β-lactoglobulin (β-LG), ovalbumin, and lysozyme. We found that with yttrium chloride, RC occurs for all proteins tested here, except lysozyme. We have also extended our experiments to different multivalent salts including $LaCl_3$, $FeCl_3$, $AlCl_3$, and spermine chloride ($SpeCl_4$). We found that $LaCl_3$, $FeCl_3$, and $AlCl_3$ also cause RC for all proteins tested except lysozyme. Here, we note that lysozyme does not show RC in any case with any salt in our experiments, and $SpeCl_4$ does not cause RC with any protein used in our experiments. The results are summarized in Table I, where "+" corresponds to the existence of RC whereas "−" represents its absence. It is worth to note that $LaCl_3$ exhibits a phase diagram very similar to YCl_3, but different from $FeCl_3$ and $AlCl_3$. Proteins with $FeCl_3$ and $AlCl_3$ exhibit a very narrow condensed regime (in comparison with YCl_3), for example, for 20 mg/mL BSA with addition of $FeCl_3$, c^* and c^{**} are ∼1.5 and ∼2.5 m*M*, respectively (Fig. 1). A typical phase diagram with $FeCl_3$ is shown in Figure 2(b).

Dependence of c and c** on protein concentration*

Using laser transmission,[6] an extended phase diagram of BSA solution with YCl_3 was obtained [Fig. 2(a)] for protein concentrations down to 0.01 m*M*. A linear relationship between c^*, c^{**}, and the protein concentration c_p was found. This observation can be made for all proteins with both YCl_3 and $LaCl_3$. The linear relationship between c^*, c^{**}, and c_p can be easily understood by assuming a near-quantitative binding of the counterions to the exposed acidic side chains. In this simple model, the exposed side chains are increasingly saturated with trivalent counterions binding to them. If the counterions bind quantitatively, each protein molecule would remove a specific number m^* of counterions from solution before the first phase transition. Increasing the salt concentration would then provide additional counterions, which also bind, until the aggregates redissolve, once m^{**} counterions are bound, and the overall interaction, thus, becomes repulsive again. With these assumptions, the two numbers m^* and m^{**} can be determined from the phase diagrams directly using the following relations.

$$\begin{aligned} c^* &= c_1 + m^* c_P \\ c^{**} &= c_2 + m^{**} c_P \end{aligned}, \qquad (1)$$

where c_1 and c_2 are constants, and m^*, m^{**} are the number of ions condensed on the surface of a protein for protein condensation and redissolution. Using rela-

Table I
The Phase Behavior of Various Protein and Salts Tested in This Work

	YCl_3	$LaCl_3$	$FeCl_3$	$AlCl_3$	$SpeCl_4$
Bovine serum albumin (BSA)	+	+	+	+	−
Human serum albumin (HSA)	+	+	+	+	−
Ovalbumin (OVA)	+	+	+	+	−
β-Lactoglobulin (β-LG)	+	+	+	+	−
Lysozyme (LYZ)	−	−	−	−	−

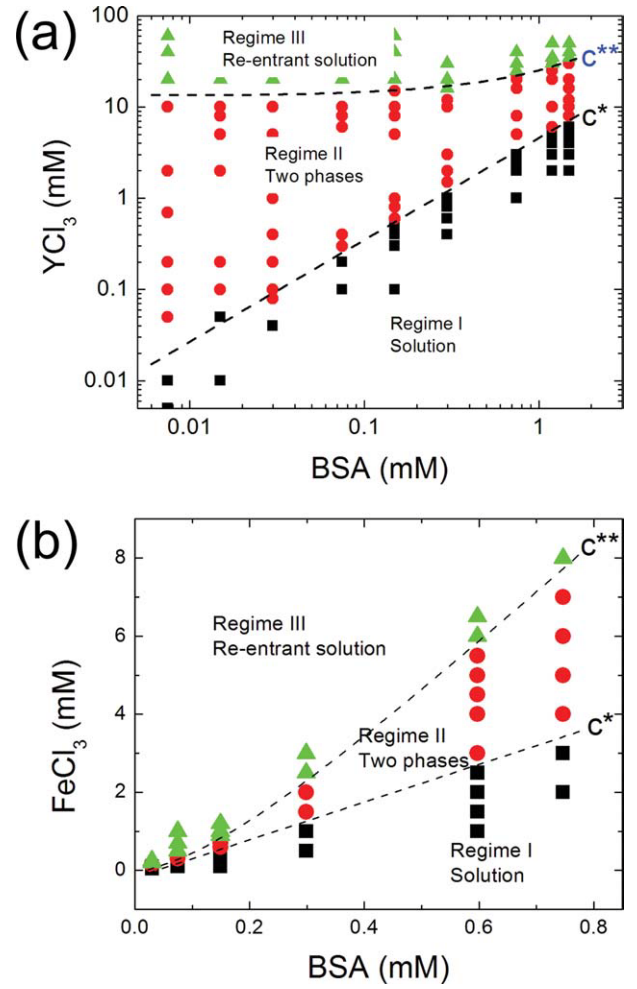

Figure 2

Extended phase diagram of BSA as a function of protein and YCl_3 on a log scale (**a**) and the phase diagram of BSA in the presence of $FeCl_3$ (**b**), which has a very narrow condensed regime II. Note the different scales in (a) and (b). [Color figure can be viewed in the online issue, which is available at wileyonlinelibrary.com.]

tion (1), we can determine m^* and m^{**}, that is, the number of ions binding to a protein and the salt concentration in the bulk solution, from the phase diagrams [Figs. 2(a,b)]. The results for BSA, ovalbumin, β-LG, and HSA are summarized in Table II. For BSA with YCl_3, we obtain $m^* = 4.3 \pm 0.5$ when proteins aggregate and $m^{**} = 15 \pm 1$ for the redissolution of the aggregates. β-LG forms dimers in solution with net charge around $-10e$ per dimer at pH 7.[37] This is the reason why the m^* value for β-LG with YCl_3 is much smaller than that of the other proteins.

In the case of protein solutions with Fe^{3+} or Al^{3+} [Fig. 2(b)], while the c^* still linearly increases with protein concentration, c^{**} exhibits a super-linear increase. The reason for this response is probably the pH change of the solution (discussed below).

Charge inversion determined by zeta potential measurements

The central mechanism during RC is charge inversion, as supported by Monte Carlo simulations below. Here, we present direct experimental evidence from electrophoretic mobility measurements.[38] Electrophoretic mobility was used to monitor the zeta potential of proteins as a function of c_{salt}. Zeta potential (ζ) distributions for protein solutions as a function of c_{salt} are narrow and shift continuously to positive surface potential. The results of ζ on two different proteins as a function of yttrium chloride concentration are presented in Figure 3. The plots of ζ–c_{salt} show a transition from negative to positive. For example, without added salt, BSA is negatively charged with $\zeta \sim -30$ mV. With increasing yttrium concentration, ζ increases and becomes positive at higher c_{salt}. The whole range can be divided into three regimes by c^* and c^{**} (Fig. 3). In all cases, c^* is very close to $\zeta \sim 0$ mV, whereas c^{**} corresponds to a significantly positive (Fig. 3). In the intermediate regime (II) defined by $c^* < c < c^{**}$, where the absolute value of ζ is small, the protein solutions are phase-separated.

It is worth noting that adding salts to protein solutions can also change the pH of the solution. We have measured the pH for the pure salt solutions. For YCl_3 and $LaCl_3$, the pH ranges between 5.5 and 6.5. Above 20 m*M*, the pH of the salt solutions remains essentially constant. The strong acidity of Fe^{3+} and Al^{3+} results in a strong pH decrease on addition of these salts: pH is in the range of 4.5–3.5 for Al^{3+} and 3.5–1.8 for Fe^{3+}. The isoelectric point (pI) of BSA is about 4.6,[39] thus, the presence of Y^{3+} or La^{3+} in solution, and the associated pH change is not enough to invert the surface charge of the protein. For Al^{3+} and Fe^{3+}, the effect might be sufficient to lead to a positive net charge, if the pH drops below the pI despite the buffering effect of the protein. To clarify this issue, we have measured the pH of a series of protein solutions with different salt concentrations around the condensed regime (Fig. 4). It is clear that the pH value ~5 for solutions at c^{**} (e.g., 5 mg/mL BSA with 2.5 m*M* $FeCl_3$) is still slightly above the pI of BSA. These measurements indicate that although the pH affects the solutions, quantitatively, it is not the main reason of charge inversion, implying cation binding must be the main driving force for charge inversion.

Monte-Carlo simulations: Comparison of the numerical and experimental results

*Prediction of the first phase boundary c**

As the simulation approach considers only a single protein structure, the resulting binding pattern corresponds to the behavior at very low protein concentration in the experimental system. For a given counterion concentration, this approximation described above (Materials

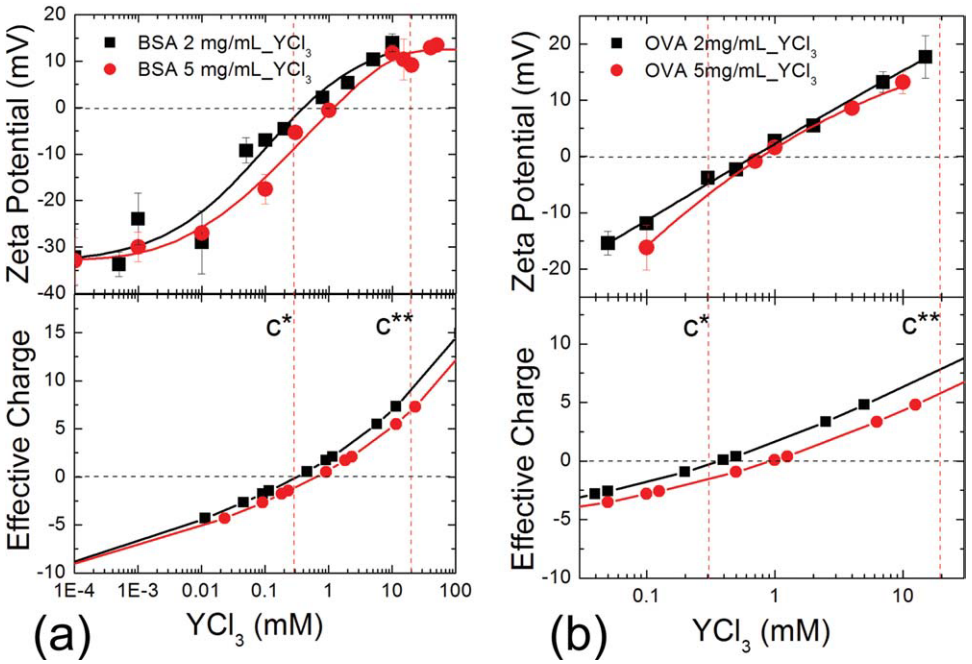

Figure 3

Comparison of experimental zeta potential values to the effective net charge of the protein by MC simulations as a function of yttrium chloride for BSA (a) and OVA (b). The c^* and c^{**} values correspond to the protein concentration of 5 mg/mL. [Color figure can be viewed in the online issue, which is available at wileyonlinelibrary.com.]

and Methods) can be considered sufficiently accurate up to a critical protein concentration $c_{crit}(P)$ at which the average electrostatic interaction energy equals about half the thermal energy. Below this concentration, protein–protein interactions can be neglected. Therefore, the critical concentration of salt needed to neutralize a single protein–ion-complex, $c_{crit}(M^{3+})$ is assumed to be correct up to this critical protein concentration $c_{crit}(P)$.

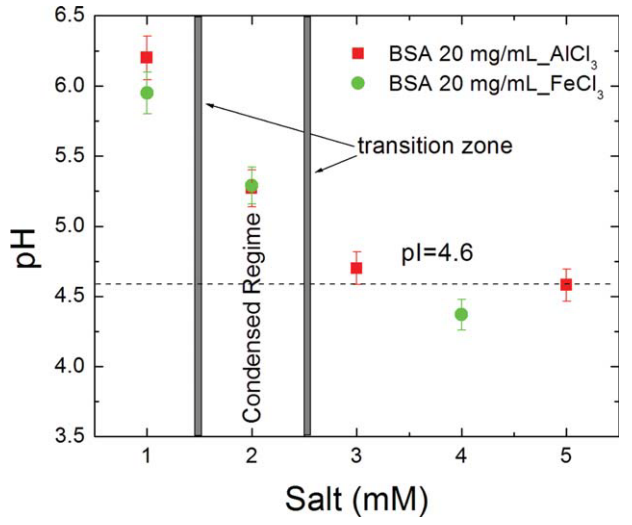

Figure 4

The pH Measurements of protein (BSA)-salt solutions around phase transitions, all pH values are above the isoelectric point of protein (4.6). BSA 20 mg/mL with $FeCl_3$, and $AlCl_3$ has a similar $c^* \sim 1.5$ m*M* and $c^{**} \sim 2.5$ m*M*. [Color figure can be viewed in the online issue, which is available at wileyonlinelibrary.com.]

Based on the observations on RC phenomena in colloidal systems, we suggest that the first phase transition occurs close to an effective charge of zero, with the corresponding counterion concentration of $c_{crit}(M^{3+})$. In this most simple model, we identify the colloidal surface charge with the overall protein charge. In the regime of low protein–protein interaction, we assume a quantitative binding of the counterions to the side chains. This implies that the curve of zero effective charge, C_M in the phase diagram is a linear function of the form $C_M = m^* c_P$ with slope of $m^* = \frac{c_{crit}(P)(M^{3+})}{c_{crit}(P)}$.

To investigate whether the charge inversion effect coincides with the outset of the aggregation regime, we compare the slope of the first phase transition curve, c^* and the predicted curve of zero effective charge C_M. As can be seen from the experiment (cf. Table II), the offset c_1 of the linear function is close to zero and thus in good agreement with the theoretical charge inversion curve. The experimental data and computationally predicted data for m^* are listed in Table II. For all proteins, our simulations predict m^* with good accuracy. This result is important as it strongly supports the notion that the determining factor is charge inversion.

Table II
Parameters of Proteins Obtained From Phase Diagram and MC Simulations for Proteins with Yttrium Chloride

Proteins	pI[a]	m*[b]	m**[b]	c_1 (m*M*)[b]	c_2 (m*M*)[b]	Initial charge	m*[c] (sim)	Number of positive/negative charged residues
BSA	4.6	4.3 ± 0.5	15 ± 1	−0.2 ± 0.2	12 ± 1	−11	4.83	80/91
HSA	4.6	3.4 ± 0.5	58 ± 2	0.1 ± 0.2	3 ± 1	−9	3.79	80/89
Ovalbumin	5.2	1.8 ± 0.2	4 ± 1	0.1 ± 0.2	24 ± 5	−8	1.82	39/47
β-LG	5.3	0.5 ± 0.2	3 ± 1	0.05 ± 0.02	0.08 ± 0.02	−10[d]	0.42	40/50
Lysozyme	10.7	–	–	–	–	–	–	–

[a]Isoelectric point of protein.
[b]Binding numbers (m^* and m^{**}) and corresponding salt concentration (c_1 and c_2) defined by Eq. 1 at phase boundaries.
[c]Binding number, m* determined by Monte Carlo simulation.
[d]Net charge for β-LG dimer in solution, see Ref. (37).

Moreover, it clarifies that the attractive force, which is finally responsible for the condensation, does not become relevant until the overall electrostatic forces are almost neutralized. The simplicity of the model (neglect of protein–protein interaction and simple estimation of the critical protein concentration) clearly confines the margin of interpretation. The good qualitative and quantitative agreement with experimental data support the specific counterion binding as the driving force of reentrant protein condensation and gives reason to believe that this is a universal phenomenon.

Qualitatively, a further binding of counterions will increase the repulsive electrostatic force that causes the proteins to redissolve. A quantitative prediction of m^{**} and c_2 remains a challenge, although. The current theoretical model does not include protein–protein interactions that are the dominating force in the region of the phase diagram where the protein precipitates. To take those interactions into account, we have to better understand the balance of attractive and repulsive interactions in the condensed phase. This is the focus of future work.

Comparison of the zeta potential and protein effective charge

The comparison with experimental zeta potential data (Fig. 3) reveals two main features: The functional form of the zeta potential and the effective protein charge exhibit similar shapes. Both ζ and the effective protein charge become zero at about the same counterion concentration. This zero point depends on the protein concentration: an increase in protein concentration is accompanied by a shift to a higher counterion concentration. This behavior is directly implied in the theoretical concept and is thus reproduced by our simulations.

DISCUSSION

RC of proteins as a universal phenomenon

Table I summarizes all systems investigated here including five different globular proteins and five different multivalent salts. In the presence of yttrium chloride, the proteins (BSA, HSA, OVA, and β-LG), which are negatively charged at neutral pH, exhibit RC. Lysozyme, which is positively charged at neutral pH, does not exhibit RC. The other conclusion we get is that trivalent ions used in this work can induce RC, but Spe^{4+}, which is a very efficient condensation agent for DNA and polyelectrolytes,[14] does not induce RC for protein solutions. This may be simply because of the low charge density, that is, the charges are so widely spread that they effectively act as singly charged counterions and hence bind nonspecifically.

The data shown so far strongly hint that the charge inversion is the driving force for RC. All proteins studied in this work (except lysozyme) have a larger number of acidic residues than negative residues and are negatively charged in solution in the absence of trivalent metal ions. This negative charge is then compensated, and finally overcompensated, during counterion addition. Thus, it is plausible to assume that it can only occur for proteins with an initial negative net charge. Lysozyme is positively charged at neutral pH, which does not show RC with any salts used in this work. To get an upper bound on the prevalence of RC, we have analyzed the number of proteins that are negatively charged through a simple statistical study. The UniRef50 database was used as a representative set of protein sequences known so far. Of the 2,867,124 sequences analyzed, 1,408,556 (46%) contain more acidic than basic residues and are, thus, negatively charged at neutral pH and in the absence of trivalent metal ions. The phenomenon of RC, thus, should be a frequently occurring phenomenon observable for nearly every second protein family.

The coupling parameter

Mean field theories (such as Debye-Hückel) intuitively lead to the introduction of a crucial length scale: the Gouy-Chapman length λ, for the thickness of the double layer that describes the adsorption of neutralizing counterions on the surface[1,2,7]

$$\lambda = \frac{1}{4\pi} \frac{q_e}{\sigma l_b Z}, \qquad (2)$$

where σ describes the surface charge, l_b is the Bjerrum length, q_e the elementary charge, and Z denotes the valence of the counterions. However, mean-field theories fail to describe the charge inversion. Manning condensation can reduce the effective surface charge of a plane or a cylinder, but it can never invert the sign of the charge.[3] The reason for this deficiency is the neglect of the pronounced correlations between the counterions—the effect indeed depends crucially on the discrete nature of the charges. A well-established theory accounting for this effect is the so-called strongly correlated liquid (SCL) theory,[7] where a second length scale competes with Eq. (2) in determining the global behavior of the system: the average distance of the discrete counterions adsorbed on the surface, *a*. Indeed, for a number of model systems—mainly planar and cylindrical systems with a uniform charge distribution—it has been shown that the ratio between these two quantities, the so-called coupling parameter defined as $\lambda = \frac{1}{4\pi}\frac{a}{\lambda}$,[7,13] allows systems that can undergo RC to be distinguished from those that cannot: a strong 2D coupling in colloid systems, i.e., $\Gamma > 2$, yields strongly attractive forces and thus leads to RC.

While this concept has been very fruitful,[7,13] in the case of proteins, as discussed in this work, the situation is fundamentally different. The length scales of ion volume, ionic screening, and charge variance on the surface of the protein are all of the same order, rendering not only the validity of mean field theories but also the applicability of SCL theory questionable. Furthermore, our experiments strongly support the idea of localized binding of the highly charged counterions to selected discrete spots on the protein surface. In this model, the bound ions cannot freely arrange on the surface. Hence, the average distance of the discrete counterions *a* should fail to describe the counterion pattern sufficiently well. Nevertheless, we note that a naive application of SCL theory to our system can still be performed: approximating the proteins as uniformly charged spheres with a suitable radius derived from their crystal structures allows a simple computation of Γ. Indeed, such an analysis shows that ~95% of all negatively charged proteins in the PDB feature $\Gamma > 2$ in this model. Whether this is a coincidence or indeed hints at a potential universality, cannot yet be decided on the basis of these data.

CONCLUSIONS AND IMPLICATIONS

RC of globular proteins in solution in the presence of multivalent metal ions is universal for acidic proteins in the presence of trivalent metal ions (Y^{3+}, La^{3+}, Fe^{3+}, and Al^{3+}). Charge inversion is indeed the major reason of redissolution of the aggregates as confirmed by zeta potential measurements. Monte Carlo simulations successfully predict the charge inversion of proteins in the presence of multivalent metal ions. The calculated binding number m^* is in good agreement with the values determined from the experimental phase diagram. Statistical estimation of the universality indicates that the phenomenon of RC could be a frequent phenomenon occurring with nearly half of all proteins in the presence of multivalent metal ions. The observations reported here provide a way to tune the protein interactions in solution and understand the role of the multivalent metal ions on the protein crystallization procedure.

REFERENCES

1. Belloni L. Colloidal interactions. J Phys Condens Matter 2000;12: R549–R587.
2. Levin Y. Electrostatic correlations: from plasma to biology. Rep Prog Phys 2002;65:1577–1632.
3. Manning GS. Counterion condensation theory constructed from different models. Phys A 1996;231:236–253.
4. Angelini TE, Liang H, Wriggers W, Wong GCL. Like-charge attraction between polyelectrolytes induced by counterion charge density waves. Proc Natl Acad Sci USA 2003;100:8634–8637.
5. Larsen AE, Grier DG. Like-charge attractions in metastable colloidal crystallites. Nature 1997;385:230–233.
6. Zhang F, Skoda MWA, Jacobs RMJ, Zorn S, Martin RA, Martin CM, Clark GF, Weggler S, Hildebrandt A, Kohlbacher O, Schreiber F. Reentrant condensation of proteins in solution induced by multivalent counterions. Phys Rev Lett 2008;101:148101.
7. Grosberg AY, Nguyen TT, Shklovskii BI. The physics of charge inversion in chemical and biological systems. Rev Mod Phys 2002;74:329–345.
8. Linse P, Lobaskin V. Electrostatic attraction and phase separation in solutions of like-charged colloidal particles. Phys Rev Lett 1999;83:4208–4211.
9. Linse P, Lobaskin V. Electrostatic attraction and phase separation in solutions of like-charged colloidal particles. J Chem Phys 2000;112:3917–3927.
10. Lobaskin V, Qamhieh K. Effective macroion charge and stability of highly asymmetric electrolytes at various salt conditions. J Phys Chem B 2003;107:8022–8029.
11. Lund M, Jönsson B. A mesoscopic model for protein-protein interactions in solution. Biophys J 2003;85:2940–2947.
12. Wu J, Bratko D, Prausnitz JM. Interaction between like-charged colloidal spheres in electrolyte solutions. Proc Natl Acad Sci USA 1998;95:15169–15172.
13. Rouzina I, Bloomfield VA. Macroion attraction due to electrostatic correlation between screening counterions. 1. Mobile surface-adsorbed ions and diffuse ion cloud. J Phys Chem 1996;100:9977–9989.
14. Bloomfield VA. DNA condensation. Curr Opin Struct Biol 1996;6:334–341.
15. Saminathan M, Antony T, Shirahata A, Sigal LH, Thomas T, Thomas TJ. Ionic and structural specificity effects of natural and synthetic polyamines on the aggregation and resolubilization of single-, double-, and triple-strands DNA. Biochemistry 1999;38:3821–3830.
16. Burak Y, Ariel G, Andelman D. Onset of DNA aggregation in presence of moonovalent and multivalent counterions. Biophys J 2003;85:2100–2110.
17. Yang J, Rau DC. Incomplete ion dissociation underlies the weakened attraction between DNA helices at high spermidine concentrations. Biophys J 2005;89:1932–1940.
18. Hsiao PY. Linear polyelectrolytes in tetravalent salt solutions. J Chem Phys 2006;124:044904.

19. Nguyen TT, Rouzina I, Shklovskii BI. Reentrant condensation of DNA induced by multivalent counterions. J Chem Phys 2000;112: 2562–2568.
20. Olvera de la Cruz M, Belloni L, Delsanti M, Dalbiez JP, Spalla O, Drifford M. Precipitation of highly charged polyelectrolyte solutions in the presence of multivalent salts. J Chem Phys 1995;103:5781–5791.
21. Solis FJ, Olvera de la Cruz M. Collapse of flexible polyelectrolytes in multivalent salt solutions. J Chem Phys 2000;112:2030–2035.
22. Shklovskii BI. Screening of a macroion by multivalent ions: correlation-induced inversion of charge. Phys Rev E 1999;60:5802–5811.
23. Butler JC, Angelini T, Tang JX, Wong GCL. Ion multivalence and like-charge polyelectrolyte attraction. Phys Rev Lett 2003;91:028301.
24. Shklovskii BI. Wigner crystal model of counterion induced bundle formation of rodlike polyelectrolytes. Phys Rev Lett 1999;82:3268.
25. Gelbart WM, Bruinsma RF, Pincus PA, Parsegian VA. DNA-inspired electrostatics. Phys Today 2002;53:38.
26. Kornyshev AA, Lee DJ, Leikin S, Wynveen A. Structure and interactions of biological helices. Rev Mod Phys 2007;79:943–996.
27. Piazza R. Interactions and phase transitions in protein solutions. Curr Opin Colloid Interface Sci 2000;5:38–43.
28. Piazza R. Protein interactions and association: an open challenge for colloid science. Curr Opin Colloid Interface Sci 2004;8:515–522.
29. Oakley AE, Collingwood JF, Dobson J, Love G, Perrott HR, Edwardson JA, Elstner M, Morris CM. Individual dopaminergic neurons show raised iron levels in Parkinson disease. Neurology 2007;68:1820–1825.
30. Selmer M, Wilting R, Holmlund D, Su X. Preparation of a crystallizable mRNA-binding fragment of moorella thermoacetica elongation factor selB. Acta Crystallogr Sect D Biol Crystallogr 2002;58:1871–1873.
31. Bouyain S, Longo PA, Li S, Ferguson KM, Leahy DJ. The extracellular region of erbB4 adopts a tethered conformation in the absence of ligand. Proc Natl Acad Sci USA 2005;102:15024–15029.
32. Bénas P, Legrand L, Riès-Kautt M. Strong and specific effects of cations on lysozyme chloride solubility. Acta Crystallogr D Biol Crystallogr 2002;58:1582–1587.
33. Li SJ. Structural details at active site of hen egg white lysozyme with di- and trivalent metal ions. Biopolymers 2006;81:74–80.
34. Schaefer M, Sommer M, Karplus M. pH-dependence of protein stability: absolute electrostatic free energy differences between conformations. J Phys Chem B 1997;101:1663–1683.
35. Weggler S, Ziller MJ, Zhang F, Schreiber F, Kohlbacher O, Hildebrandt A. Monte Carlo simulation of multivalent metal ion-protein binding. J Phys Chem B, in preparation.
36. Ianeselli L, Zhang F, Skoda MWA, Jacobs RMJ, Martin RA, Callow S, Prévost S, Schreiber F. Protein-protein interactions in ovalbumin solutions studied by small-angle scattering: effect of ionic strength and the chemical nature of cations. J Phys Chem B 2010;114:3776–3783.
37. Elofsson UM, Paulsson MA, Arnebrant T. Adsorption of β-lactoglobulin A and B in relation to self-association: effect of concentration and pH. Langmuir 1997;13:1695–1700.
38. Besteman K, Van Eijk K, Lemay SG. Charge inversion accompanies DNA condensation by multivalent ions. Nat Phys 2007;3:641–644.
39. Zhang F, Skoda MWA, Jacobs RMJ, Martin RA, Martin CM, Schreiber F. Protein interactions studied by SAXS: effect of ionic strength and protein concentration for BSA in aqueous solutions. J Phys Chem B 2007;111:251–259.